INS/GNSS Localization Using 15 State Extended Kalman Filter

Mushfiqul Alam, Gines Moreno, Martin Sipos, Jan Rohac

Czech Technical University in Prague, Department of Measurement, Faculty of Electrical Engineering
Technicka 2, Prague, CZECH REPUBLIC
Corresponding Author: mushfala@fel.cvut.cz

Abstract

MEMS (micro-electro-mechanical system)-based inertial sensors, i.e., accelerometers and angular rate sensors, are commonly used as a cost-effective solution for the purposes of navigation in a broad spectrum of application like RPAS (Remotely Piloted Aircraft System), surface vehicles or even mobile phones. Even if MEMS sensors have an advantage in their size, cost, weight and power consumption, they suffer from bias instability, noisy output and insufficient resolution. Multi-sensor data fusion aided with GNSS measurement are usually used for providing accurate navigation solution. The performance of the estimation algorithms is often dependent on the dynamic behavior of the vehicle. In the presented paper, an extend Kalman filter (EKF) based fusion algorithm is used for the navigation solution of a high-speed boat, and an aircraft which exhibits rapidly changing dynamic conditions. The aim of this paper is to propose a novel EKF architecture to estimate the position, velocity, attitude of a fast moving boat and aircraft while estimating accelerometer and angular rate sensor's bias. A novel 15 state EKF architecture is presented in the paper and compared with the currently existing commonly used 12 state EKF architecture. The performance of the newly proposed EKF is validated using high-speed boat experiment in the sea. The results demonstrated significant improvement in the estimation performance and confirmed the suitability of the new 15 state EKF.

1. Introduction

A strapdown MEMS based low cost inertial measurement unit (IMU) are commonly used for localization problem in various vehicles such as lightweight aircraft, high-speed boat, unmanned aerial vehicles (UAV), etc. For localization a strapdown inertial system consisting of tri-axial accelerometers (ACC) and tri-axial gyros is commonly used for attitude estimation (roll, pitch, yaw angle) as well as for velocity and position evaluations. For precise measurements, ring laser gyros and servo ACCs are used on board onboard any vehicles, which is expensive. In comparison, MEMS sensors are compact, lightweight, and cost effective thus offering a cheap solution for navigation purposes. However, at the same time MEMS based inertial sensors suffer from bias instability, insufficient sensitivity, noise etc., which present significant challenges in data processing that have to be dealt with in navigation processes [1], [2]. Originally, the attitude, velocity and position are supposed to be evaluated by integrating angular rates from gyros and ACC; nevertheless, as aforementioned the measurements suffer from several inaccuracy impacts. Thus this integration causes unbounded error growth in the estimation process, which is corrected by additional aiding measurements such as GNSS (Global Navigation Satellite System) forming a complete inertial navigation system (INS) [3], [4]. The error in GNSS measurement does not depend on time, thus making suitable as an aiding source. The main drawbacks of MEMS inertial sensors are their bias instability. Therefore, for vehicles which exhibits high dynamic motion, it is essential to estimate the biases in the sensors [5].

There are several approaches for fusing INS/GNSS in order to obtain attitude, velocity and position estimates, such as Kalman filters (KF) with nonlinear extensions of various architectures [6], [7], eXogenous Kalman Filters (XKF) and nonlinear observers [8]. Due to the dynamic motion, of a majority of vehicles, being highly nonlinear, the most commonly used approaches utilize extended Kalman filter (EKF). Ref [9], [10], [11] and [12] presented an INS/GNSS fusion architecture using EKF. The presented EKF architecture did not include the estimation of ACC bias. For vehicles going rapid dynamic changes, it is essential to estimate ACC bias for accurate estimation since ACCs are subjected to significant external forces due to high speed/ fast motion. Hence in the presented work, we propose an extension to the originally 12 state EKF proposed in [9], [10] to 15 state EKF including ACC biases. Thus the novelty of the paper lies in proposing a 15 state INS/GPS localization algorithm using EKF.

The proposed algorithm is verified using data from high speed boat experiment in order to check its performance under different kind of dynamics. After that the strength and weakness of the algorithm with respect GPS data outage is analyzed and extracted in conclusions. Rest of the paper is organized as follows, Section 2 presents details of INS/GNSS navigation principles. Section 3 presents the new proposed EKF algorithm followed by results and discussion of the experiment in Section 4. Finally, Section 5 ends with concluding remarks.

2. INS/GGNSS navigation

A. *Inertial Navigation System (INS) model*

The localization problem of a vehicle based on the EKF used needs one core-sensing device for the physicalmathematical model, which is the IMU. This unit measures the specific force applied to the vehicle in the body frame (sf_x, sf_y, sf_z), which is the addition of every acceleration, and the angular rates (p, q, r) of the vehicle with a high update rates. These data can be processed, transformed and fuse to provide the position (X, Y, Z), velocity (u, v, w), and attitude (θ,ϕ,ψ). The model used in EKF with the INS, is defined as follows.

$$\begin{cases} \dot{x}(t) = f(x(t), u(t), t) \\ y(t) = h(x(t), g(t), t) \end{cases} \tag{1}$$

$$x = \left[X, Y, Z, u, v, w, \theta, \phi, \psi, b_{gx}, b_{gy}, b_{gz}, b_{ax}, b_{ay}, b_{az}\right]^T \tag{2}$$

$$u = \left[sf_x, sf_y, sf_z, p, q, r\right]^T \tag{3}$$

$$y = [X, Y, Z, u, v, w]_{GPS}{}^T \tag{4}$$

Here x is the state vector, that contains position, velocity, Euler angles and gyroscope and accelerometer biases, u represent IMU outputs, y measurement vector and g the GPS output.

Adding accelerometer and gyroscopes biases into the state equation, their drift along time can be estimated and taken into account for more accurate and stable navigation estimation. This increases the stability of the estimation algorithms during the GPS outage. Inclusion of the velocity received from the GNSS measurement as corrective measurement, state vector's estimation has been demonstrated to be closer to the reference and more stable as well. GPS velocity has been used when vehicle velocity is higher than 3 m/s due to its lower precision under that threshold.

Navigations equations require at least two different reference frames. One fixes to the vehicle that has not relative rotation to it, which will be denoted body frame, and other fixes to the gravity center of the body but it keeps without rotation. X axis point to north, Y to east and Z to Earth center, because of that it will be denoted NED frame (North-East-Down). Position estimation and GPS signals are referred to NED frame but velocity (u, v, w) estimation and INS output are in body frame.

B. Motion equations

Euler angle rates $\dot{\theta}, \dot{\phi}, \dot{\psi}$ can be calculated directly using the following expression [9] where gyroscopes biases have been taken into account.

$$\begin{bmatrix} \dot{\theta} \\ \dot{\theta} \\ \dot{\psi} \end{bmatrix} = \begin{bmatrix} 1 & \sin(\phi)\tan(\theta) & \cos(\phi)\tan(\theta) \\ 0 & \cos(\phi) & -\sin(\phi) \\ 0 & \sin(\phi)\sec(\theta) & \cos(\phi)\sec(\theta) \end{bmatrix} \cdot \left(\begin{bmatrix} p \\ q \\ r \end{bmatrix} - \begin{bmatrix} b_{gx} \\ b_{gy} \\ b_{gz} \end{bmatrix} \right) \tag{5}$$

Assuming that the IMU is placed at the vehicle's center of gravity, vehicle acceleration is given by following equation. As velocity is referred to the body frame this acceleration has to be referred to it. First term is gravity acceleration in body frame, the second is the accelerometers measurement corrected with estimated biases and the last one is centrifugal acceleration [10].

$$\begin{bmatrix} \dot{u} \\ \dot{v} \\ \dot{w} \end{bmatrix} = C_{bn}{}^T \begin{bmatrix} 0 \\ 0 \\ g \end{bmatrix} + \left(\begin{bmatrix} sf_x \\ sf_y \\ sf_z \end{bmatrix} - \begin{bmatrix} b_{ax} \\ b_{ay} \\ b_{az} \end{bmatrix} \right) + \begin{bmatrix} vr - wq \\ -ur + wp \\ uq - vp \end{bmatrix} \tag{6}$$

C_{bn} is the Direct Cosine Transform matrix that rotates a vector from body frame to NED frame.

$$C_{bn} = \begin{bmatrix} \cos\phi\cos\theta & \sin\theta\sin\psi\cos\phi - \sin\phi\cos\psi & \sin\psi\sin\phi + \cos\phi\cos\psi\sin\theta \\ \cos\theta\sin\phi & \cos\psi\cos\phi + \sin\phi\sin\psi\sin\theta & \sin\theta\sin\psi\sin\phi - \cos\phi\sin\psi \\ -\sin\theta & \cos\psi\sin\theta & \cos\psi\cos\theta \end{bmatrix} \tag{7}$$

Lastly, velocity as position derivative has the following expression. Position is referred to NED frame so transformation is needed.

$$\begin{bmatrix} \dot{X} \\ \dot{Y} \\ \dot{Z} \end{bmatrix} = C_{bn} \begin{bmatrix} u \\ v \\ z \end{bmatrix} \tag{8}$$

Biases are model as constant over time, which varies negligibly over time.

$$\begin{bmatrix} \dot{b}_{gx} \\ \dot{b}_{gy} \\ \dot{b}_{gz} \end{bmatrix} = \begin{bmatrix} \dot{b}_{ax} \\ \dot{b}_{ay} \\ \dot{b}_{az} \end{bmatrix} = 0 \tag{9}$$

These derivatives are introduced in (1) and state vector in the next time instant is calculated. Summarizing these equations, the state model is given by the next expression.

$$f(x, u, t) = \begin{cases} C_{bn} \begin{bmatrix} u \\ v \\ z \end{bmatrix} \\ C_{bn}{}^T \begin{bmatrix} 0 \\ 0 \\ g \end{bmatrix} + \left(\begin{bmatrix} sf_x \\ sf_y \\ sf_z \end{bmatrix} - \begin{bmatrix} b_{ax} \\ b_{ay} \\ b_{az} \end{bmatrix} \right) + \begin{bmatrix} vr - wq \\ -ur + wp \\ uq - vp \end{bmatrix} \\ \begin{bmatrix} 1 & \sin(\phi)\tan(\theta) & \cos(\phi)\tan(\theta) \\ 0 & \cos(\phi) & -\sin(\phi) \\ 0 & \sin(\phi)\sec(\theta) & \cos(\phi)\sec(\theta) \end{bmatrix} \cdot \left(\begin{bmatrix} p \\ q \\ r \end{bmatrix} - \begin{bmatrix} b_{gx} \\ b_{gy} \\ b_{gz} \end{bmatrix} \right) \\ \begin{bmatrix} 0 \\ 0 \\ 0 \end{bmatrix} \\ \begin{bmatrix} 0 \\ 0 \\ 0 \end{bmatrix} \end{cases} \tag{10}$$

The observation model, h, is not as simple matrix, due to velocity in state and measurement vector are in different reference frames they are connected by a rotation matrix.

$$h(x, g, t) = \begin{bmatrix} 1 & 0 & 0 & 0 & 0 & 0 & 0 & 0 & 0 & 0 & 0 & 0 & 0 & 0 & 0 \\ 0 & 1 & 0 & 0 & 0 & 0 & 0 & 0 & 0 & 0 & 0 & 0 & 0 & 0 & 0 \\ 0 & 0 & 1 & 0 & 0 & 0 & 0 & 0 & 0 & 0 & 0 & 0 & 0 & 0 & 0 \\ 0 & 0 & 0 & & & & 0 & 0 & 0 & 0 & 0 & 0 & 0 & 0 & 0 \\ 0 & 0 & 0 & & C_{bn}{}^T & & 0 & 0 & 0 & 0 & 0 & 0 & 0 & 0 & 0 \\ 0 & 0 & 0 & & & & 0 & 0 & 0 & 0 & 0 & 0 & 0 & 0 & 0 \end{bmatrix} \tag{11}$$

Small errors in sensors will be integrated and could make estimations very inaccurate. Therefore, INS requires another system reliable enough that provides additional information to reduce these errors. GNSS measurement unit is used with INS in the fusion algorithm proposed in section 3.

Global Navigation Satellite System (GNSS)

In this section it is only written a brief description of GNSS functioning. Further information can be found in [5], [9] and [13]. GNSS uses a ranging technique from GPS satellite constellation, which is broadcasting their estimate position. These signals reached the user receiver to estimate the distance between satellites and the vehicle. With four or more satellites receiver location is obtained due to triangulation. GPS position is more reliable than INS, on the other hand its update range is much lower and signal could be loose due to natural or artificial obstacles.

3. Extended Kalman Filter

When data from different sensors are available, fusion algorithm are adopted as a scheme to obtain vehicle state. The Kalman Filter is a very effective stochastic estimator for a large wide problem variety. In general Kalman filter is used when a state is affected to random disturbance during its evolution following an equation motion. The linear model are generally not valid, physical model is nonlinear and Euler angles are not small, because of that Extended Kalman Filter (EKF) is proposed [9], [10] and [14]. When the filter operates properly, error around estimated solution is maintained reasonably small. Nevertheless, if it is not due to miss-modeling, incorrect covariance matrices tuning or initialization error it will affect the estimation. This phenomenon is known as divergence.

System is written as a nonlinear discrete time state transition, where *f* and *h* functions have been defined in (10) and (11) [15].

$$x_k = x_{k-1} + f(x(k-1), u(k-1), k-1)\Delta t \tag{1}$$

$$\begin{cases} x_k = f(x_{k-1}, u_{k-1}, w_{k-1}) \\ \quad y_k = h(x_k, v_k) \end{cases} \tag{12}$$

Here x_k is the state at time step k, w_k is some additive noise, y_k is the observation made at time k, v_k is some kind of additive observation noise. In EKF is assumed that these noises are uncorrelated zero-mean Gaussian with known covariance Q_k and R_k. Only continuous Q_c covariance matrix is known so has to be discretized.

In order to linearize the state equation around $x_{k-1} = \hat{x}_{k-1}^{+}$ and making $w_{k-1} = 0$ could be obtained.

$$\begin{aligned} x_k &= f_{k-1}(\hat{x}_{k-1}^{+}, u_{k-1}, 0) + \left.\frac{\partial f_{k-1}}{\partial x}\right|_{\hat{x}_{k-1}^{+}} (x_{k-1} - \hat{x}_{k-1}^{+}) \\ &\quad + \left.\frac{\partial f_{k-1}}{\partial w}\right|_{\hat{x}_{k-1}^{+}} w_{k-1} \\ &= f_{k-1}(\hat{x}_{k-1}^{+}, u_{k-1}, 0) + F_{k-1}(x_{k-1} - \hat{x}_{k-1}^{+}) + L_{k-1}w_{k-1} \\ &= F_{k-1}x_{k-1} + \bar{u}_{k-1} + \bar{w}_{k-1} \end{aligned} \tag{13}$$

Here F_k is the Jacobian matrix of the new state with respect to state components, $\bar{u}_{k-1}$ is the known signal, $\bar{w}_{k-1}$ is the noise signal and L_k is partial derivative of system equation f with respect to process noise w_k.:

$$F_{k-1} = \left.\frac{\partial f_{k-1}}{\partial x}\right|_{\hat{x}_{k-1}^{+}} \tag{14}$$

$$L_{k-1} = \left.\frac{\partial f_{k-1}}{\partial w}\right|_{\hat{x}_{k-1}^{+}} \tag{15}$$

$$\bar{u}_{k-1} = f_{k-1}(\hat{x}_{k-1}^{+}, u_{k-1}, 0) - F_{k-1}\hat{x}_{k-1}^{+} \tag{16}$$

$$\bar{w}_{k-1} \sim L_k Q_k {L_k}^T \tag{17}$$

If the same procedure is followed with the observation equation around $x_k = \hat{x}_k^{-}$ and making $v_k = 0$, could be obtained.

$$\begin{aligned} y_k &= h_k(\hat{x}_k^{-}, 0) + \left.\frac{\partial h_k}{\partial x}\right|_{\hat{x}_k^{-}} (x_k - \hat{x}_k^{-}) + \left.\frac{\partial h_k}{\partial v}\right|_{\hat{x}_k^{-}} v_k \\ &= h_k(\hat{x}_k^{-}, 0) + H_k(x_k - \hat{x}_k^{-}) + M_K v_k \\ &= H_k x_k + z_t + \bar{v}_k \end{aligned} \tag{18}$$

Here H_k is the matrix that correspond to $h(x_k, v_k)$, M_k is partial derivative of measurement function h with respect to measurement noise, z_k is the known signal, $\bar{v}_k$ is the noise signal of the measurements.

$$H_k = \left.\frac{\partial h_k}{\partial x}\right|_{\hat{x}_k^{-}} \tag{19}$$

$$M_K = \left.\frac{\partial h_k}{\partial v}\right|_{\hat{x}_k^{-}} \tag{20}$$

$$z_k = h_k(\hat{x}_k^{-}, 0) - H_k\hat{x}_k^{-} \tag{21}$$

$$\bar{w}_{k-1} \sim M_k R_k {M_k}^T \tag{22}$$

EKF is written as a predictor-corrector scheme where first estimation of the next step is calculated $\hat{x}_{k+1}$ and then measurements are used to obtain the final estimation.

Prediction update:

$$\hat{x}_{k/k-1} = f\left(\hat{x}_{k-1/k-1}, u_{k-1}\right) \tag{23}$$

$$Q_k = 0.5 \cdot \left(F_k G_k Q_c {G_k}^T + G_k Q_c {G_k}^T {F_k}^T\right)\Delta t \tag{24}$$

$$P_{k/k-1} = F_k P_{k-1/k-1} {F_k}^T + L_k Q_k {L_k}^T \tag{25}$$

Here G_k is the matrix that adapt matrix dimension in order to Q_k is 15x15 matrix, Δt is the time step in every prediction that is fixed by the IMU rate and P_k is the estimation error covariance matrix at step k.

Correction update:

$$\hat{y}_k = y_k - h\left(\hat{x}_{k/k-1}\right) \tag{26}$$

$$S_k = H_k P_{k/k-1} {H_k}^T + M_k R_k {M_k}^T \tag{27}$$

$$K_k = \left(P_{k/k-1} {H_k}^T\right) / S_k \tag{28}$$

$$P_{k/k} = (I - K_k H_k) P_{k/k-1} \tag{29}$$

$$\hat{x}_{k/k} = \hat{x}_{k/k-1} + K_k \hat{y}_k \tag{30}$$

In the previous equations y_k are measurements from GPS signal, $\hat{y}_k$ are the innovation or measurements residual, S_k is innovation covariance, K_k is the Kalman gain, $P_{k/k}$ corrected estimation error covariance matrix and $\hat{x}_{k/k}$ is the final state estimation after correction.

EKF is based in Taylor series expansion around the filtered and predicted estimations, assuming that errors between real state and estimated are small [10]. As high terms in this expansion have been neglected because Jacobian matrices are small could have poor performances when system was strongly nonlinear.

4. Experimental Results and Discussion

This section discusses the results obtained from an experiment in order to validate the proposed filtering algorithm. Experiment performed and used with this purpose consists in three straight lines with a high speed boat in Trondheim fjord.

Fig 1. Boat used to perform the validation experiment

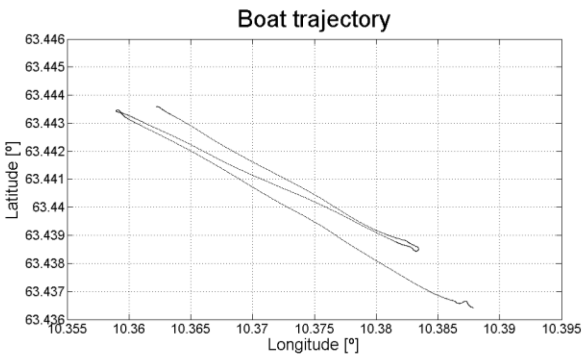

Fig 2. Boat trajectory during experiment

The sampling rates used for each sensor are *fINS=200Hz, fGPS=5Hz, fEKF=200Hz.*

Results of estimation with the EKF have been compared with the position obtained from absolute GPS measurements and with true reference position obtained from Real Time Kinematic (RTK) GPS based measurements which are more accurate. The estimation errors are calculated with respect to the reference position estimated using RTK.

A. *Position (x,y,z)*

A comparison between the EKF estimation, absolute GPS signal based position and reference RTK based GPS signal has been done and showed in the following figures, Fig 3, Fig 4, Fig 5. Position estimation frame is in NED. Due to the proximity of the three graphs a zoom section has been represented instead the whole experiment.

As can be seen from Fig 3 and Fig 4, EKF estimation is very close to GPS signal and deviations between them are very small, on the order of few centimeters. The reason of that is the trust put in GPS measurement in Q-R tuning. Furthermore, they are close to the reference signal, but shifted. This made a deviation in order of meters. Nevertheless, position in Z is less smooth and accurate than in the other axes due to errors in GPS signal used to correct the predicted estimation. These readings in the final part of the experiment reach heights of -5m, which is not possible in a boat sailing in an equipotential surface as the sea is.

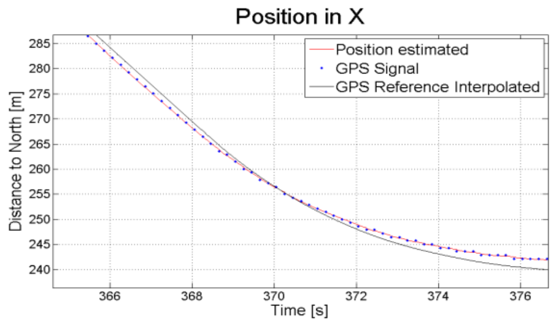

Fig 3. Zoom of position X estimation

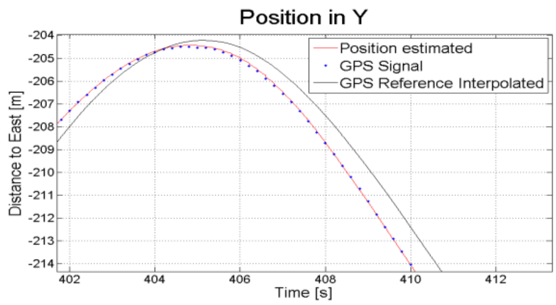

Fig 4. Zoom of position Y estimation

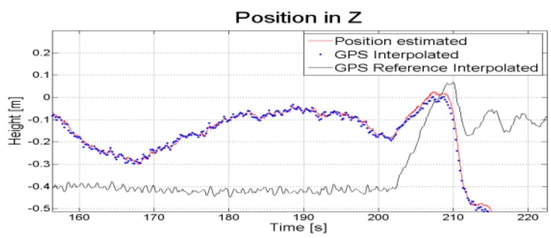

Fig 5. Zoom of position Y estimation

	Pos x [m]	Pos Y [m]	Pos Z [m]
Estimation RMSE	2,69	5,08	2,82

Table 1. Estimation Root Mean Square Error with reference position

RMSE of every position component has been calculated and summarized in Table 1, where can be seen how precise the estimation for the whole experiment is.

B. Velocity (u,v,w)

In this section comparison just includes EKF estimation and the GPS signal used to correct the predicted estimation. Reference does not provide velocity data, therefore is not possible obtain any kind of error because there is no signal to compare with. Velocity has been calculated in body frame. Again graphs show a zoom of the experiment, in the first straight line, in order to appreciate better the differences.

As in position estimation is very close to GPS signal, although velocities estimation oscillates more with a relatively high frequency. The reason of that is the Q-R tuning to achieve white noise shape innovations. Longitudinal velocity reaches the 30knots, which was the boat speed. Lateral velocity is not zero because of sea movement and sideslip. Vertical velocity to down in body frame is positive and has the same shape of longitudinal velocity because of the boat positive pitch.

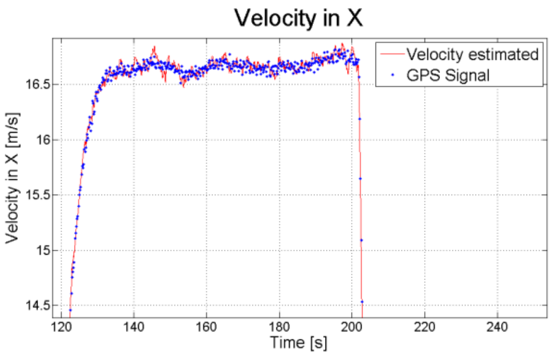

Fig 6. Zoom in the first straight line of Velocity X estimation

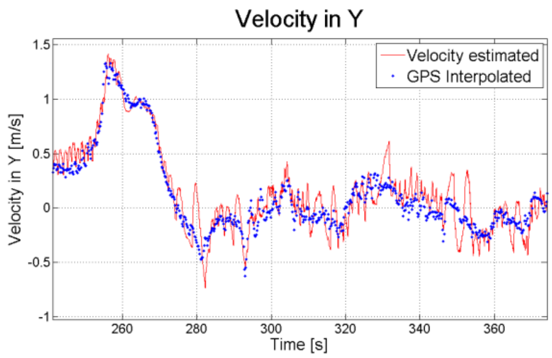

Fig 7. Zoom in the first straight line of Velocity Y estimation

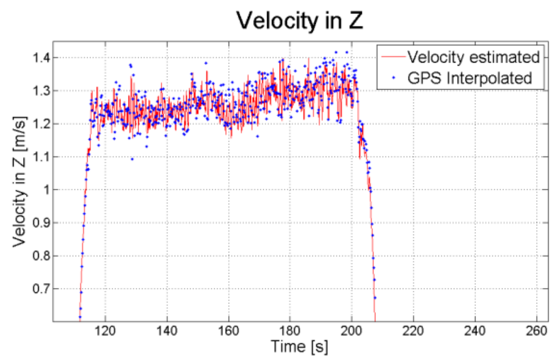

Fig 8. Zoom in the first straight line of Velocity Z estimation

C. Euler Angle (θ,ϕ,ψ)

Euler Angles estimation has been obtained but the only signal with could be compared is the one integrated from the gyroscopes, or the one obtained using the accelerometers to estimate roll and pitch. Signal directly integrated from the gyros, angles obtained by accelerometers signal assuming static conditions and EKF estimation have been plotted.

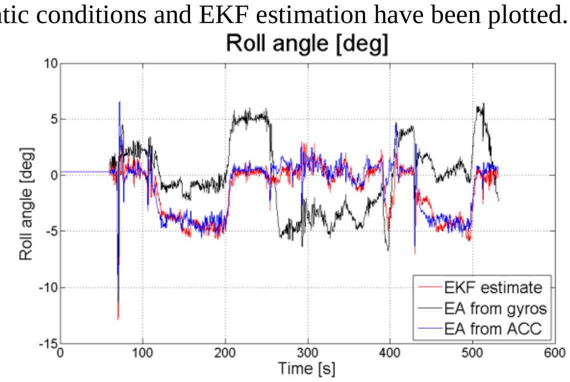

Fig 9. Roll angle estimation

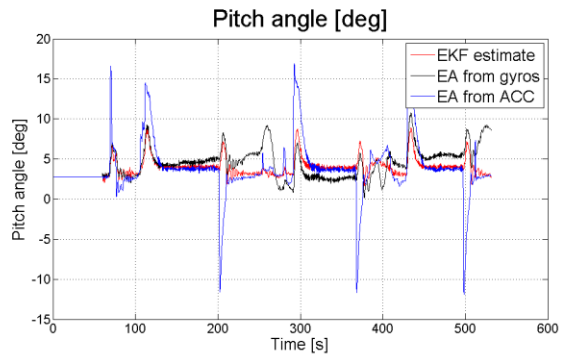

Fig 10. Pitch angle estimation

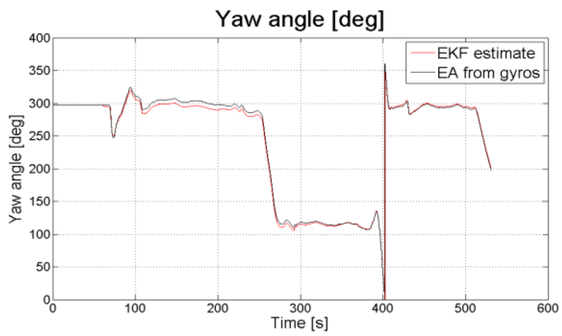

Fig 11. Yaw angle estimation

As is obvious Euler angles do not fit to estimation due to their bias. However, could be seen as the trend is roughly the same in roll and pitch graph. In yaw graph, estimation and free integration of gyro signal are much closer and are only shifted. Yaw angle cannot been obtained from accelerometers using gravity acceleration, but pitch and roll angles have demonstrated be very close to estimation in the periods of time where the boat could be considerate under static conditions.

D. Sensor biases

As sensor biases have been calculated in state vector they will be shown in the following graphs. Both biases should be stabilized and converge to a certain value between the datasheet values, because if not, it means that the code is not stable.

As can be seen in the following biases graphs, Fig

13 and Fig 12, they are stabilized in the sensors datasheet range. All of them after different periods of time converge to some value inside the range mentioned.

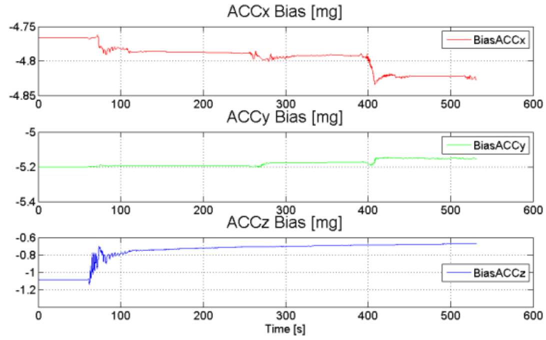

Fig 12. Accelerometer bias estimation

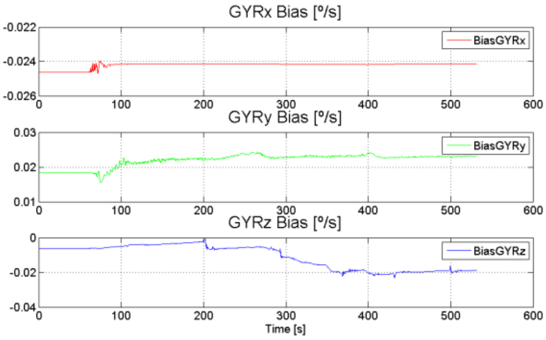

Fig 13. Gyroscopes bias estimation

E. Position and Velocity innovations

Finally, position and velocity innovations will be shown in the following graphs in order to check that they are white noise shaped and the algorithm is well tuned.

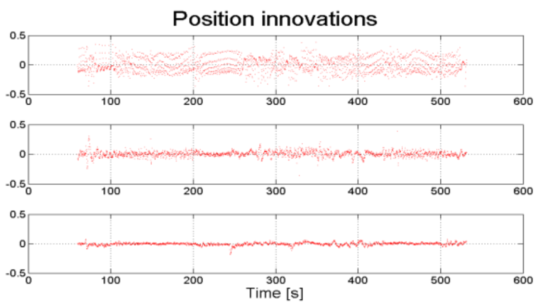

Fig 14. Position innovations

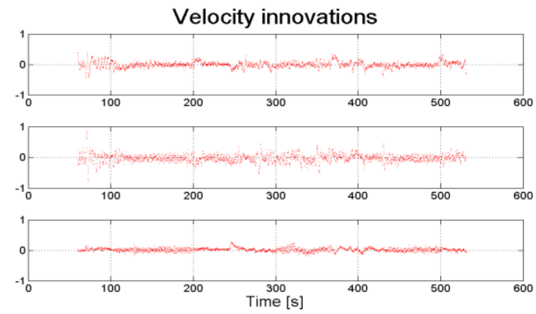

Fig 15. Velocity innovations

Both graphs contains X, Y, and Z innovations of position and velocity in their reference frame respectively. It is clearly seen how all of them look like white noise, with some oscillations and different amplitude, and are centered in zero. Therefore, can be guessed that algorithm is working properly and is well tuned. Q-R tuning is a very time-consuming task because it has to be made manually and there is not a defined process to follow it.

F. Effect of GPS signal outage

In this section has been done a research in order to verify EKF performances when the GPS signal is lost during a certain period of time. In some terrestrial vehicles GPS signal can be lost due to natural or artificial obstacles and in flight vehicles in low altitude flights as well. For that reason position estimation has to be stable enough to not be dangerous. It is also a way to check algorithm stability.

GPS has been switched off artificially 20 seconds in the second straight line. As in the previous graphs only a section of the experiment has been represented to appreciate better the differences.

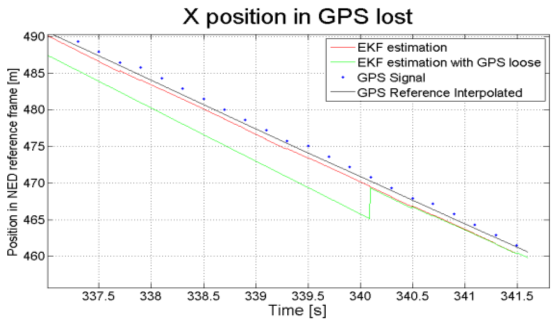

Fig 16. Comparison between X position estimation when GPS signal is lost 20 seconds

Comparison between estimation with GPS available and not, shown how estimation is diverging slowly when there are not corrective measurements. This happens in every position, velocity and Euler angles estimation, however, drift is seen more clearly in position.

	RMSE (m)	Final deviation (m)
Error in position	0.423	6.018

Table 2. Error between estimation with GPS available in every moment and estimation with GPS signal loose

This comparison during time when GPS is lost, shows how during this period of time error is growing exponentially until a maximum of 6 meters. This deviation at the end could mean a potential risk for the vehicle in where the units are located. As better units and algorithm are as precise and stable would be the estimation even without corrective measurements.

5. Conclusions

In this paper we proposed an EKF to estimate the location, velocity and attitude of any vehicle using INS/GPS measurements. It has demonstrated to provide an accurate and stable position, velocity and attitude estimation with a RSME of 6.4 m when estimation is compared with the reference RTK based GPS positioning. Algorithm has demonstrated estimate accelerometers and gyroscopes bias and keep them in datasheet ranges as well. Position and velocity innovations and their white noise shaped show the well tuning of the EKF algorithm.

An addition research for stability has been performed switching off 20 seconds the GPS signal artificially. During that experiment it has demonstrated how position estimation given only by IMU signal and free integration without correction diverges slowly until reach a maximum deviation of 6.018m. This slow deviation indicates the well biases estimation and could be acceptable for some applications.

Acknowledgement

The work of the authors were partially supported by the Czech Technical University in Prague under internal grant No. SGS15/163/OHK3/2T/13 and the EEA/Norway grant No. NF-CZ07-ICP-3-2082015 supported by the Ministry of Education, Youth and Sports of the Czech Republic, titled “Enhanced Navigation Algorithms in Joint Research and Education”.

References

[1] M. Alam, M. Sipos, J. Rohac and J. Simanek, "Calibration of a Multi-sensor Inertial Measurement Unit with Modified Sensor Frame," in *International Conference Industrial Technology (ICIT)*, Sevilla, Spain, 2015.

[2] M. Alam and J. Rohac, "Adaptive Data Filtering of Inertial Sensors with Variable Bandwidth," *Sensors,* vol. 15, no. 2, pp. 3282-329, 2015.

[3] M. Park, Error Analysis and Stochastic Modeling of MEMS based Inertial Sensors for Land Vehicle Navigation Applications, Calgary: The University of Calgary, 2014.

[4] J. Farrell, Aided Navigation: GPS with High Rate Sensors, New York: McGraw Hill Education, 2008.

[5] K. Dmitrieva, P. Segall and C. DeMets, "Network-based estimation of time-dependent noise in GPS position time series," *Journal of Geodesy,* vol. 89, no. 6, pp. 591-606, 2015.

[6] J. Simanek, M. Reinstein and V. Kubelka, "Evaluation of the EKF-Based Estimation Architectures for Data Fusion in Mobile Robots," 2014.

[7] D. Simon, "Kalman filtering with state constraints: a survey of linear and nonlinear algorithms," *IET Control Theory \& Applications,* vol. 4, no. 8, pp. 1303-1318, 2010.

[8] T. A. Johansen and T. I. Fossen, "The eXogenous Kalman Filter (XKF)," *International Journal of Control,* pp. 1-7, 2016.

[9] N. Abdelkrim and N. Aouf, "Robust INS/GPS Sensor Fusion for UAV Localization Using SDRE Nonlinear Filtering," *IEEE Sensors Journal,* vol. 10, no. 4, pp. 789-798, 2010.

[10] N. Abdelkrim, N. Aouf, A. Tsourdos and B. White, "Robust nonlinear filtering for INS/GPS UAV localization," in *16th Mediterranean Conference on Control and Automation*, Ajaccio, France, 2008.

[11] B. Ristic, S. Arulampalam and N. Gordon, Beyond the Kalman filter, pertical filters for tracking applications, Artech House, 2004.

[12] M. Reinstein and V. Kubelka, "Complementary filtering approach to orientation estimation using inertial sensors only," in *IEEE International Conference on Robotics and Automation (ICRA)*, Prague, Czech Republic, 2012.

[13] E. D. Kaplan and C. J. Hegarty, Understanding GPS, Pinciples and Applications, London: Artech House, 2006.

[14] D. J. I. G. Mora, "Filtro de Kalman para problemas de Dinámica relativa," Madrid, 2015.

[15] J. O. S. I. Luis Sánchez, "Extended Kalman filter and extended particle Kalman filter for non linear estimation problems," *Revista Ingeniería UC,* vol. 20, no. 1, pp. 7-16, 2013.